



Predicting Intraserotypic Recombination in Enterovirus 71

Andrew Woodman,^a Kuo-Ming Lee,^b Richard Janissen,^c Yu-Nong Gong,^b Nynke H. Dekker,^c Shin-Ru Shih,^{b,d,e,f}
Craig E. Cameron^a

^aDepartment of Biochemistry and Molecular Biology, The Pennsylvania State University, University Park, Pennsylvania, USA

^bResearch Center for Emerging Viral Infections, Chang Gung University, Taoyuan, Taiwan

^cDepartment of Bionanoscience, Kavli Institute of Nanoscience, Delft University of Technology, Delft, The Netherlands

^dDepartment of Medical Biotechnology and Laboratory Science, College of Medicine, Chang Gung University, Taoyuan, Taiwan

^eDepartment of Laboratory Medicine, Linkou Chang Gung Memorial Hospital, Taoyuan, Taiwan

^fResearch Center for Chinese Herbal Medicine, Research Center for Food and Cosmetic Safety, and Graduate Institute of Health Industry Technology, College of Human Ecology, Chang Gung University of Science and Technology, Taoyuan, Taiwan

ABSTRACT Enteroviruses are well known for their ability to cause neurological damage and paralysis. The model enterovirus is poliovirus (PV), the causative agent of poliomyelitis, a condition characterized by acute flaccid paralysis. A related virus, enterovirus 71 (EV-A71), causes similar clinical outcomes in recurrent outbreaks throughout Asia. Retrospective phylogenetic analysis has shown that recombination between circulating strains of EV-A71 produces the outbreak-associated strains which exhibit increased virulence and/or transmissibility. While studies on the mechanism(s) of recombination in PV are ongoing in several laboratories, little is known about factors that influence recombination in EV-A71. We have developed a cell-based assay to study recombination of EV-A71 based upon previously reported assays for poliovirus recombination. Our results show that (i) EV-A71 strain type and RNA sequence diversity impacts recombination frequency in a predictable manner that mimics the observations found in nature; (ii) recombination is primarily a replicative process mediated by the RNA-dependent RNA polymerase; (iii) a mutation shown to reduce recombination in PV (L420A) similarly reduces EV-A71 recombination, suggesting conservation in mechanism(s); and (iv) sequencing of intraserotypic recombinant genomes indicates that template switching occurs by a mechanism that may require some sequence homology at the recombination junction and that the triggers for template switching may be sequence independent. The development of this recombination assay will permit further investigation on the interplay between replication, recombination and disease.

IMPORTANCE Recombination is a mechanism that contributes to genetic diversity. We describe the first assay to study EV-A71 recombination. Results from this assay mimic what is observed in nature and can be used by others to predict future recombination events within the enterovirus species A group. In addition, our results highlight the central role played by the viral RNA-dependent RNA polymerase (RdRp) in the recombination process. Further, our results show that changes to a conserved residue in the RdRp from different species groups have a similar impact on viable recombinant virus yields, which is indicative of conservation in mechanism.

KEYWORDS conservation, EV-A71, predictive, replicative recombination

The *Enterovirus* genus in the family *Picornaviridae* currently consists of 15 species. Outside rhinoviruses, the enteroviruses responsible for human mortality and morbidity fall specifically into groups A, B, C, and D (1, 2). This group of viruses, typified by poliovirus (PV), has a 7.5-kb positive-sense RNA genome that encodes a single polyprotein that is flanked by noncoding regions. The polyprotein is co- and posttransla-

Citation Woodman A, Lee K-M, Janissen R, Gong Y-N, Dekker NH, Shih S-R, Cameron CE. 2019. Predicting intraserotypic recombination in enterovirus 71. *J Virol* 93:e02057-18. <https://doi.org/10.1128/JVI.02057-18>.

Editor Julie K. Pfeiffer, University of Texas Southwestern Medical Center

Copyright © 2019 American Society for Microbiology. All Rights Reserved.

Address correspondence to Andrew Woodman, auw23@psu.edu, or Craig E. Cameron, cec9@psu.edu.

Received 19 November 2018

Accepted 19 November 2018

Accepted manuscript posted online 28 November 2018

Published 5 February 2019

tionally processed by virus-encoded proteases to generate the structural proteins (VP4, VP2, VP3, and VP1), which assemble to form the icosahedral capsid and the nonstructural proteins (2A^{Pro}, 2B, 2C, 3A, 3B^{VPg}, 3C^{Pro}, and 3D^{Pol}) that mediate replication of the virus genome (3).

RNA viruses, like those found in the *Enterovirus* genus, exist as a viral quasispecies as a consequence of misincorporations by their error-prone RNA-dependent RNA polymerases (RdRps) during genome replication (4, 5). In addition, recombination enables the exchange of genetic material through a proposed “copy choice” mechanism in which the viral RdRp, along with the nascent RNA, switches templates during replication, creating hybrids between two viruses replicating in the same cell (6–8). As well as being a driver of genetic variation, it is believed that recombination may have evolved in order to “rescue” genomes from deleterious mutations that accumulate during error-prone replication (9).

Enterovirus 71 (EV-A71), a member of the species A group, is an important neurotropic enterovirus for which there is currently no effective therapy or vaccine and manifests most frequently as a childhood illness known as hand, foot, and mouth disease (HFMD) (10). However, acute EV-A71 infection can also be associated with flaccid paralysis, myocarditis, or even fatal encephalitis (10, 11). EV-A71 variants have been classified into three groups (GgA, GgB, and GgC), and recombination has been linked to the founding of each subgroup lineage (12). More importantly, cocirculation of the species A EV-A71 and coxsackievirus A16 (CV-A16) viruses has been associated with large-scale outbreaks of HFMD (13, 14). Sequence analysis of clinical isolates obtained since 2008 from patients with fatal neurological symptoms has demonstrated that these cases are mainly due to subgenogroup C4 of EV-A71, which was previously identified as an EV-A71/CV-A16 recombinant virus (15, 16). In related enteroviruses, recombinant forms defined by serotype according to their capsid proteins, have been shown to emerge, prevail, and then disappear in temporal epidemiological surveys of globally distributed serotypes (12, 17, 18). In many of these examples, the recombinants are pathogenic.

It is evident that recombination is a critical driver of virus evolution with medically important consequences. While the triggers and mechanisms of recombination in PV are starting to be understood (19–21), the ability to predict the likelihood of a recombination event between circulating viruses of public health relevance has not been available. We wanted to use the cell-based approaches that have been developed to study recombination in PV as a tool to test whether recombination events for EV-A71 in cell culture mimic what is observed in nature (22). In order to study recombination in EV-A71, we have developed a robust, reproducible cell-based assay. The established *in vitro* assay based upon the previously reported assays for PV (19–21) consists of two genomes, each containing a different deleterious (and nonreverting) modification that prevents the production of viable progeny. Only a recombination event between the two genomes can produce viable virus. Current investigations of PV recombination have shown that targeted mutations to the RdRp of the donor and acceptor templates can significantly alter the yield of recombinant virus (19, 21). We introduced a similar RdRp mutation (L420A in PV and L421A in EV-A71) into our cell-based recombination assay and demonstrate a significant reduction in recombinant yield. The same mutation had no impact on replication but led to an EV-A71 virus population that was ultrasensitive to the antiviral ribavirin. We expanded our assay to consider the role of cell-mediated nonreplicative recombination since this pathway is known to occur for PV (23, 24). Our results indicate that only a minor amount of EV-A71 recombinant virus is produced via this mechanism, further supporting the interpretation that recombination is primarily RdRp mediated. Crucially, we tested the biological relevance of our assay by expanding it to include two additional circulating strains of EV-A71: a strain known to recombine (C4) and a strain that is not recombinogenic (B5). Our results show important significant differences in viable recombinant virus yield that mimic observations found in nature. Limited sequencing of recombinant genomes suggested that no sequence motif acted as a trigger for recombination, but it did show

that RNA sequence complementarity at the recombination site may be important, adding support to the widely accepted “copy choice” mechanism of template switching. We believe that this assay can be used as a tool to predict the likelihood of recombination between current circulating EV-A71 strains.

(This article was submitted to an online preprint archive [25].)

RESULTS

Development of an EV-A71 cell-based recombination assay. In order to predict recombination events in EV-A71 an experimental system is required. The study of viral factors that modulate enterovirus recombination have benefited from the recent development of recombination specific cell-based assays in PV that use parental templates that are only able to produce viable virus via recombination (19–21). A suitable “donor” template for the assay was the already-established subgenogroup C2 EV-A71 (TW/2231/98) subgenomic replicon, where a firefly luciferase reporter replaces the entire P1 region (26) (Fig. 1A). We modified the replicon by engineering a hammerhead ribozyme immediately 5′ of the internal ribosomal entry sequence (IRES), a change that would ensure an authentic genomic sequence following *in vitro* RNA transcription (27). The modification led to a significant improvement in replication in human embryonic rhabdomyosarcoma (RD) cells with a 3-log_{10} increase in reporter signal (a surrogate marker for genome replication) compared to the unmodified replicon (data not shown). One recently used assay for the study of PV recombination, known as CRE-REP (20), uses an acceptor template that has characterized mutations within the 2C Oril stem-loop that inhibits positive-sense RNA synthesis (28, 29). The EV-A71 Oril has not been fully characterized so similar mutations to the predicted stem-loop in 2C were not considered. In addition, mutations to the Oril of the related coxsackievirus B3 have been shown to revert, or produce virus with 5′ RNA truncations (30, 31). The “acceptor” template in our assay was the EV-A71 C2-MP4 strain (32) that had a region removed within the 3D coding region of the genome that encompasses the active site of the RdRp (EV-A71 Δ 3D), similar to an acceptor template used in a PV model for recombination (21). After cotransfection of donor and acceptor RNA templates into permissive cells, a viral-RdRp-mediated template switch from donor to acceptor may produce a fully functional recombinant genome (Fig. 1A). Cell-based studies on the dynamics of EV-A71 replication are primarily carried out in RD or African green monkey (Vero) cells, which are susceptible to EV-A71 infection due to the expression of the receptor SCARB2 (33). Since enterovirus recombination has been shown to be a replicative process (19–21), we wanted to select a cell type for any EV-A71 recombination assay that would be optimal for replication of the donor replicon template. We initially quantified the luciferase signal, a marker for RNA replication, at 8 h after the transfection of RD and Vero cells with the EV-A71 C2 replicon RNA. The results indicated that Vero cells were suboptimal for any future recombination assays as the luciferase signal was significantly lower (nearly 2 log_{10}) than that produced in the RD cell line (data not shown). A subsequent cotransfection of RD cells with donor and acceptor RNA templates in equimolar ratios yielded viable recombinant virus (8.8×10^3 PFU/ml $\pm 2 \times 10^3$) (Fig. 1B), an amount in line with previous studies that used PV as a model (19–21). Transfection of the donor and acceptor RNA templates alone produced no viable virus (Fig. 1B). To ensure that the observed virus was recombinant and to gain insight into the location of template switching, individual viruses were plaque purified and subjected to reverse transcription-PCR (RT-PCR) sequence analysis. Both donor and acceptor templates are derived from the EV-A71 subgenogroup C2 parental strains and share high sequence similarity (99.3% at the RNA level). Precise identification of the site of recombination would therefore be difficult. In two examples (Fig. 1C), the location of recombination was shown to fall within the 2A region. The first recombinant has a junction that falls within a 34-nucleotide window of shared homology between donor and acceptor templates. Similarly, the second recombinant has a junction that falls within a larger, 248-nucleotide window. Importantly, all isolated sequences were recombinant, validating the experimental approach.

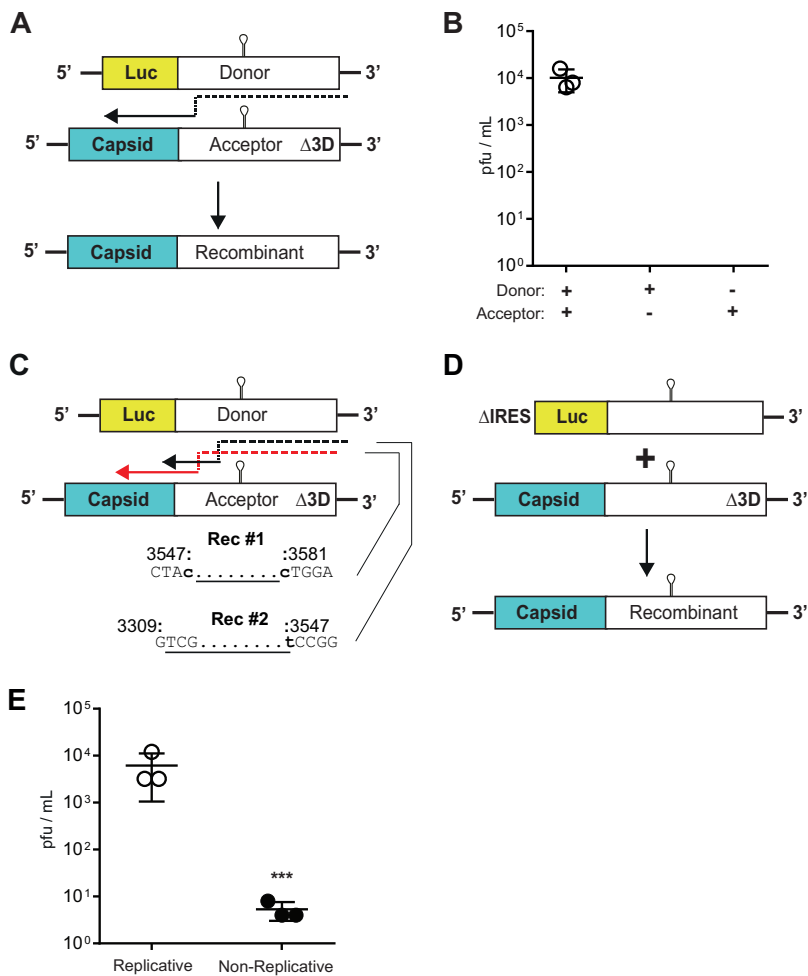


FIG 1 Enterovirus 71 (EV-A71) recombination in RD cells is primarily replicative. (A) Cell-based EV-A71 recombination assay. C2 strain firefly luciferase-encoding subgenomic replicon (donor) and full-length EV-A71 C2-MP4 strain genome (acceptor) carrying a lethal deletion of the 3D^{pol} region were cotransfected in an equimolar ratio into RD cells. A fully functional virus genome can be produced via an RdRp template switch from donor to acceptor (indicated by dashed black arrow). (B) Only upon cotransfection can replication-competent virus be generated (PFU/ml \pm standard deviations [SD]; $n = 3$) (C) Example sequences of plaque-purified recombinant virus from C2/C2 (left panel). Dashed arrows indicate predicted paths of viral RdRp upon template switching. Numbering refers to the position upon the acceptor templates. Lowercase, boldface nucleotides indicate the 5' and 3' boundaries of recombination. The underlined sequences indicate region of homology. (D) Nonreplicative recombination assay. IRES deletion of the C2 donor template inhibits translation. The acceptor template remains the same as in panel A. Viable virus will only be produced via a cell-mediated event. (E) Yield of recombinant virus (PFU/ml \pm SD; $n = 3$) originating from transfection in equimolar ratio of replicative and nonreplicative partners. Statistical analyses were performed using an unpaired, two-tailed t test (***, $P = 0.0001$).

EV-A71 recombination is primarily a replicative process. We generated an additional parental genome that would be unable to replicate in order to confirm whether the recombination we were observing was from a replicative process and therefore different from nonreplicative recombination (23, 34–36). We removed the entire IRES from the EV-A71 C2 subgenomic replicon producing the C2-ΔIRES replicon template. This inhibits the translation of the viral RNA, ensuring that no active RdRp is produced (Fig. 1D). The second RNA partner in this “nonreplicative” assay was the same acceptor template shown in Fig. 1A (EV-A71Δ3D). Importantly, both templates carried the relevant coding sequences that would produce a viable virus if a nonreplicative mechanism of recombination occurred (Fig. 1D). In a side-by-side experiment with the replicative recombination assay (Fig. 1A), equimolar ratios of replicative partners and the newly developed nonreplicative partners were transfected into RD cells. Quantifi-

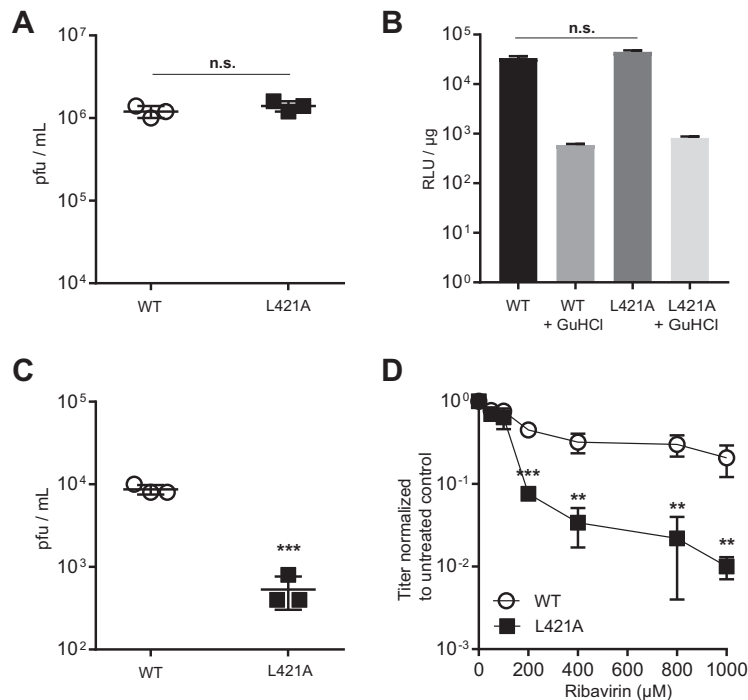


FIG 2 Mutation to the donor RdRp inhibits recombination and increases susceptibility to ribavirin. (A) L421A mutation does not impact virus yield. Yields of virus are shown for wild-type EV-A71 C2-MP4 and the L421A variant after transfection of RNA (PFU/ml \pm SD; $n = 3$). (B) L421A mutation does not impact donor template replication. Cells were transfected with 250 ng of wild-type EV-A71 replicon and the L421A variant with or without 4 mM guanidine hydrochloride. The luciferase activity is reported in relative light units (RLU) per microgram of total protein in the extract at 8 h posttransfection. (C) L421A inhibits EV-A71 replicative recombination. Yields of recombinant virus following transfection of either wild-type or L421A variant donor template with acceptor RNA in RD cells were determined (PFU/ml \pm SD; $n = 3$). Statistical analyses were performed using an unpaired, two-tailed t test (***, $P = 0.0003$). (D) EV-A71 L421A population is highly susceptible to ribavirin. RD cells were infected at an MOI 0.1 with wild-type or L421A variant EV-A71 C2-MP4 virus in the presence of various concentrations of ribavirin. After achieving a CPE, virus supernatant was clarified and used for a plaque assay. Results show titer of virus normalized to an untreated control (PFU/ml \pm SD; $n = 3$). Statistical analyses were performed using an unpaired, two-tailed t test (***, $P = 0.0004$; **, $P < 0.005$).

cation of virus at 60 h posttransfection showed that the replicative partners were able to produce significantly more viable recombinant virus (5.4×10^3 PFU/ml $\pm 2 \times 10^3$) compared to the nonreplicative assay (~ 10 PFU/ml) (Fig. 1E). This result is highly suggestive that recombination in EV-A71 is primarily a replicative process that is RdRp mediated, similar to that observed for PV (19–21).

An RdRp mutation impairs recombination but not replication. Current investigations of PV recombination have shown that targeted mutations to the RNA-dependent RNA polymerase (RdRp) can have a significant impact upon the yield of recombinant virus (19–21). An L420A change within the RdRp coding region has been shown to significantly inhibit recombination in a PV model (21). The leucine residue is conserved in the prototype strains of EV-A, -B, -C, and -D (position 421 of the RdRp coding region in EV-A71). We therefore reasoned that if the underlying mechanism(s) of recombination were conserved between enterovirus species, a similar modification to the RdRp of the donor template might inhibit recombination in the newly developed EV-A71 recombination assay. We first introduced the L421A modification into the EV-A71 C2-MP4 full-length clone and quantified virus production after transfection of RNA into RD cells. No significant difference in virus yield was observed compared to the wild type (Fig. 2A). In addition, the luciferase signal with or without guanidine hydrochloride of the L421A C2 replicon template was similar to the wild-type replicon at 8 h posttransfection (Fig. 2B). Taken together, the two experiments demonstrated that the L421A variant has no negative impact upon replication, an important prerequisite for

interpretation of any recombination assay. We then carried out a recombination assay to investigate the impact of the L421A mutation on virus yield. After transfection of wild-type parental RNA, an average recombinant yield of 8.6×10^3 PFU/ml ($\pm 1 \times 10^3$ PFU/ml) was observed. In contrast, when the L421A mutation was present in the RdRp donor template the yield of recombinant was significantly reduced by >10-fold, measuring an average of 5.3×10^2 PFU/ml ($\pm 2 \times 10^2$ PFU/ml) (Fig. 2C). Recombination has been proposed as an adaptive mechanism that generates combinations of beneficial mutations and/or removal of deleterious mutations that may appear in a population of viruses after replication (37, 38). If this hypothesis is correct, then a virus population that is unable to “purge” deleterious mutations via recombination should be highly susceptible to mutagenic compounds such as nucleoside analogues. Indeed, a population of PV carrying the L420A mutation has been shown to be highly susceptible to the mutagen ribavirin (21). Kempf et al. proposed that this is not related to RdRp fidelity but rather a direct result of inhibiting recombination. We tested an EV-A71 population carrying the similar L421A mutation. RD cells were infected at a multiplicity of infection (MOI) of 0.1 in the presence of increasing concentrations of ribavirin. Viable virus was then quantified by PFU and normalized to an untreated control. The results showed that concentrations of ribavirin of $>200 \mu\text{M}$ led to a significant decrease in the viability of the L421A EV-A71 population compared to wild-type (Fig. 2D). Importantly, the results with the L421A variant further support the interpretation that recombination in EV-A71 is a replicative process and potentially indicate that the mechanism(s) of recombination and the consequences thereof in enteroviruses may indeed be conserved across species groups.

Use of alternate donor templates significantly impacts recombinant virus yield in a predictive manner. The main goal of developing the EV-A71 recombination assay was to test its predictive power in reproducing what is observed in nature. In order to do this, two additional subgenomic replicons (donor templates) were engineered and introduced into the assay. Importantly, both donor templates were developed from the current circulating clinical isolates TW-00073-2012 and TW-50144-2013, with phylogenetic analysis placing them within the C4 and B5 subgenogroups, respectively (Fig. 3). At the RNA level, the donor replicon C4 and B5 strains both share ~80% RNA sequence homology with the acceptor template C2 strain within the region of recombination (Table 1). The majority of nucleotide differences are, however, at the wobble-base position since the amino acid homology to the acceptor template is ~95% for both replicon strains (Table 1). Importantly, current phylogenetic data show the C4 group has evolved by genetic shift through intra- and intertypic recombination events. Indeed, the C4 subgenotype is characterized by a higher similarity to the prototype CV-A16 virus (G-10) at the P2 and P3 region (Fig. 3, marked in green). In contrast, analysis of B5 members clusters them in an independent clade within the genotype B group and suggests that evolution has been limited to genetic drift only (Fig. 3, orange arrow). Since the B5 subgenogroup is not associated with current circulating recombinant viruses, we hypothesized that the B5 donor template in our recombination assay may produce significantly lower recombinant yield compared to the C2 and C4 donor templates. A single-step growth curve for the EV-A71 C4 and B5 clinical isolates indicated no significant difference in replication (Fig. 4A). In addition, we tested the replication kinetics of the new subgenomic replicons using a luciferase time course assay (Fig. 4B). The results show a similar luciferase signal as a function of time for all three donor templates, with the B5 replicon producing a marginally higher reporter signal at each time point compared to the C2 and C4 strains. Because there was no significant difference in replication between the three donor templates, a subsequent recombination assay was carried out for each pairing. Quantification of recombinant virus showed that alternate donor templates did indeed significantly impact viable recombinant yield (Fig. 4C). All of the combinations tested produced detectable virus ($\text{C2/C2} = 6.9 \times 10^3$ PFU/ml $\pm 2.4 \times 10^3$, $\text{C4/C2} = 4.2 \times 10^2$ PFU/ml $\pm 10^2$, and $\text{B5/C2} = 5.6 \times 10^1$ PFU/ml ± 10), and all of the viruses produced were recombinant (see representative sequences in Fig. 4D and E). If RNA sequence homology is the driving

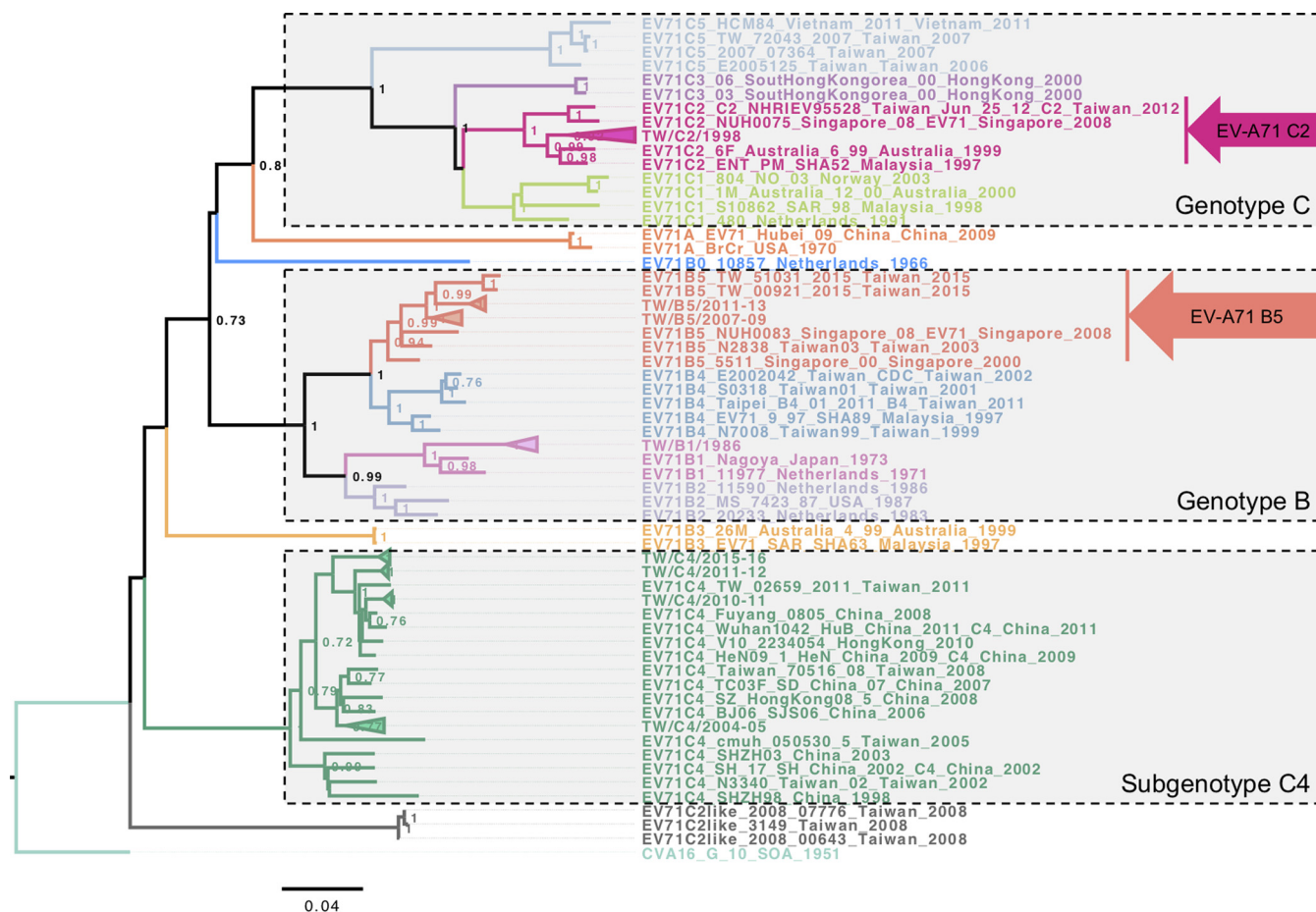


FIG 3 Phylogenetic analysis of EV-A71 genotypes B and C. Neighbor-joining phylogenetic analysis of EV-A71 genotypes B and C was based on their P2-P3 genome region, rooted by the coxsackievirus (CV) A16 prototype strain G10 (isolated in 1951). The subtrees show mixed clusters of evolutionary intra- and intertypic recombination events of analyzed EV-A71 sequences ($n = 182$). EV-A71 subgenotypes and genotypes are depicted in different colors. The subgenotype B5 (orange arrow) is located within the genotype B cluster, showing a ladder-like evolutionary scale. In contrast to other subgenotypes of genotype C, the subgenotype C4 (labeled in green) forms an outgroup of genotype C, close to other recombinogenic EV-A71 strains (e.g., B3 and C2-like) and the prototype CV-A16 sequence. The probabilities of replicate trees in which associated taxa clustered together in the bootstrapped data (1,000 replicates) are shown next to the branches. The phylogenetic tree is drawn to scale, with branch lengths representing the numbers of base substitutions per site.

force for RdRp mediated “copy choice” recombination, then the significantly higher yield for the C2/C2 partners compared to the other two conditions is not surprising, given the RNA sequence homology between donor and acceptor templates is >99%. However, the C4 and B5 replicons shared similar divergence in RNA sequence to the acceptor, but the yield of recombinant virus was significantly different. This result indeed followed what is observed in nature and suggests that the *in vitro* cell-based assay has some power for predicting the efficiency of EV-A71 intraserotypic recomb-

TABLE 1 Nucleotide and amino acid identity between donor template (C4 and B5 strains) and acceptor template (C2 strain)^a

EV-A71 strain	Sequence type	Identity (%)											
		Overall	VP4	VP2	VP3	VP1	2A	2B	2C	3A	3B	3C	3D
C4	Nucleotide	83.3	88.9	91.3	91.9	90.5	84.9	74.7	79.0	76.4	75.8	75.8	77.9
	Amino acid	96.7	100.0	100.0	99.6	98.7	97.3	92.9	96.7	94.2	90.9	94.0	93.9
B5	Nucleotide	80.1	80.7	81.2	82.0	83.1	81.2	75.8	79.7	78.1	80.3	77.3	79.1
	Amino acid	95.5	100.0	97.6	97.1	97.3	96.7	91.9	95.7	93.0	95.5	91.8	93.7

^aConsensus sequences of the C4 and B5 subgenotypes were used to perform the pairwise sequence alignments with the C2 acceptor template strain. The EV-A71 full-genome sequences used to calculate the consensus are described by Lee et al. (22). The sequence identities at the RNA and amino acid levels are denoted as percentages. Boldfacing indicates sequence identities at the RNA level to the C2 acceptor template in the region where recombination can occur.

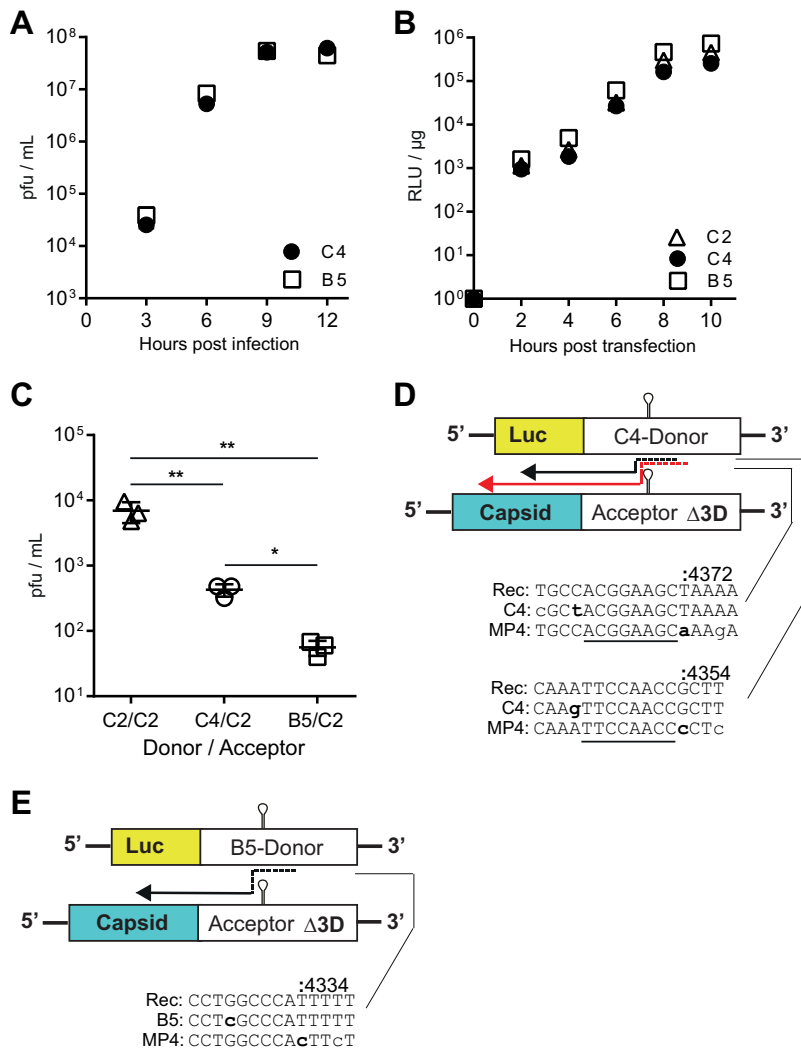


FIG 4 Alternate donor templates significantly impact viable recombinant frequency in a predictable manner. (A) Single-step growth curve at an MOI 10 of EV-A71 C4 and B5 strains shows no significant difference in replication. (B) C2, C4, and B5 subgenomic replicon firefly luciferase time courses. Cells were transfected with 250 ng of each respective EV-A71 replicon, and the luciferase activity is reported in RLU per microgram of total protein in the extract. (C) EV-A71 recombination assay. RD cells were transfected with the various EV-A71 subgenomic replicon donors and EV71Δ3D RNA. The results show the yield of recombinant virus (PFU/ml ± SD; $n = 3$). Statistical analyses were performed using an unpaired, two-tailed t test (**, $P < 0.01$; *, $P < 0.05$). (D and E) Representative recombinant sequences of plaque-purified recombinant virus from C4/C2 (E) and B5/C2 (F). Dashed arrows indicate predicted paths of viral RdRp upon template switching. Numbering refers to the position on the acceptor templates. Lowercase, boldface nucleotides indicate the 5' and 3' boundaries of recombination. Underlined sequences indicate regions of homology.

nation. We concluded that subtle underlying differences at either the RNA or proteome level inhibit recombination with B5 subgenogroup members. Experiments to characterize these differences are ongoing.

Isolated recombinant viruses show homology at the recombination junction(s) and that the trigger for recombination is sequence independent. The exact location of recombination from the primary C2/C2 recombinant viruses isolated in this study was impossible to identify due to the high sequence similarity of the two parental templates (Fig. 1C). Since the C4 and B5 templates had ~20% divergence at the RNA level within the P2 and P3 regions, where template switching would occur (Table 1), identification of recombinant junction would in principle be easier. Of note, only one independent B5/C2 recombinant sequence was identified (Fig. 4E). Because the yield of

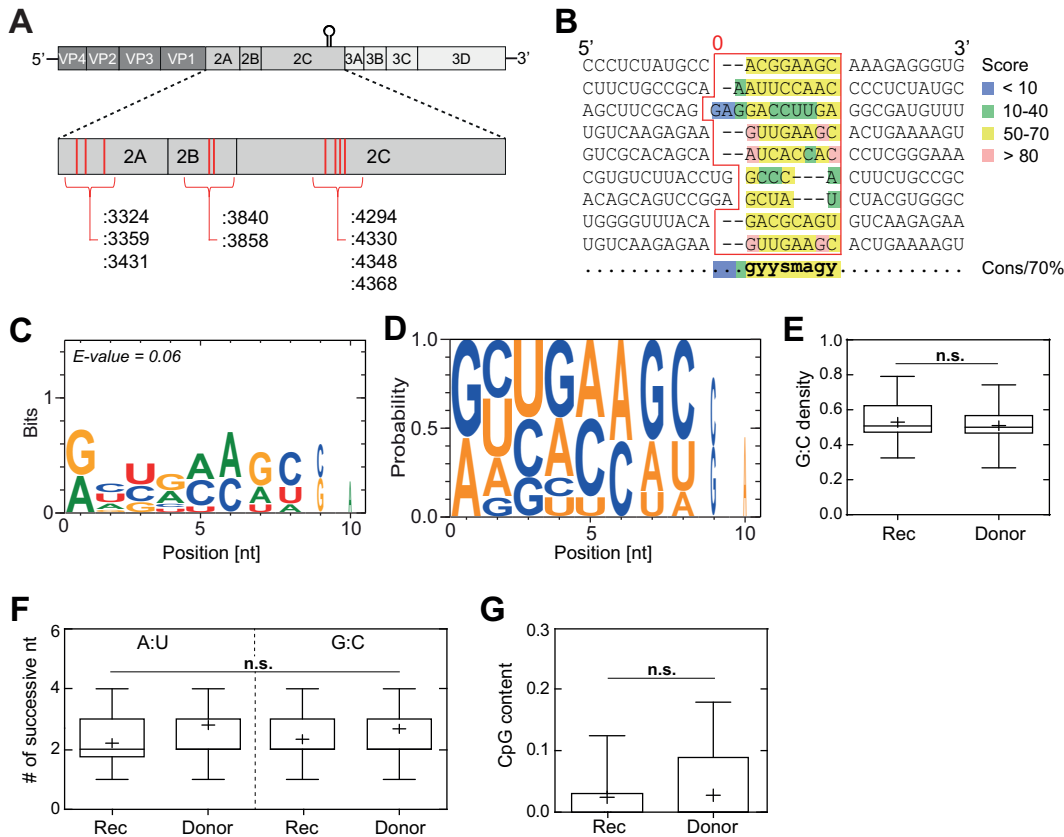


FIG 5 Intraserotypic recombination between EV-A71 C2 and C4 subgenotypes requires homology at the recombination junction, but the triggers for template-switching are sequence independent. (A) Positions of template-switching events observed during intratypic recombination between the EV-A71 C2 and C4 subgenotypes. The individual positions of observed strand switching across the P2 genome region are marked in red, including their corresponding nucleotide sequence numbers with respect to the C2 acceptor strand. (B) Sequences of bona fide C2/C4 recombinant viruses. The red border highlights the matching homologous sequences at the recombination sites with lengths between 5 and 11 nucleotides ($\bar{x} = 7 \pm 2$ nucleotides). The sequences were subject to M-COFFEE, a multiple sequence alignment algorithm, to identify possible gapped sequence motifs. Scores of <50 are considered to exhibit poor sequence consistency (scores range from 0 to 100). The sequence homology for the matching homologous sequences was found to be $58\% \pm 2\%$. A consensus sequence with 70% probability is shown below using IUPAC nomenclature. (C) Logo of ungapped *de novo* sequence motif search using the MEME algorithm that represents a sequence-aligned, position-dependent nucleotide probability matrix. The resulting motif sequence with an E value of 0.06 and a bit value of <1 show no statistical significance and thus failed to find a sequence motif as a recombination trigger. (D) Probability of position-dependent nucleotides at the homologous recombination sequences without sequence alignment. (E to G) The G-C nucleotide density (E), numbers of successive G-C/A-U bases (F), and CpG contents (G) of the homologous recombination sequences and the entire C2 genome (10-nucleotide sequence window) exhibit no significant differences. Statistical analysis was performed using a one-way, two-tailed analysis of variance with comparative Tukey *post hoc* test (n.s., not significant).

recombinant virus from this combination was very low (mean, 5.6×10^1 PFU/ml), this finding may be unsurprising and may represent the sole recombinant in the population. The C4/C2 intraserotypic pairing provided more viable recombinants which were subsequently used for sequence analysis. Plaque purified viruses were characterized by RT-PCR analysis in a window between the end of P1 and P2 (Fig. 5A). All recombinant viruses identified were derived from the parental genomes, as expected. In all examples, a region of between 5 and 11 nucleotides of shared homology between donor and acceptor templates was identified at the recombination junction with no insertions or deletions (Fig. 5A). The identified homologous sequences shared a sequence homology of only $58\% \pm 2\%$ and were subject to *de novo* sequence motif search to identify possible conserved sequences that may trigger the observed recombination events. Potentially, the cell-based recombination assay only provides information of secondary recombination products that do not necessarily represent the primary recombinant product, so we hypothesized that these may still share similar sequence motifs, if any

exist. We first analyzed the identified sequences with M-COFFEE (39), a multiple sequence alignment algorithm that allows gaps between sequence regions (Fig. 5B) to allow best alignment. The computation was set to combine the following alignment algorithms: MAFFT, ClustalW, DIALIGN-TX, POA, MUSCLE, T-COFFEE, PCMA, and PROBCONS. The algorithm was not able to identify a highly conserved sequence motif, and the proposed consensus sequence with a probability of 70% only exhibited a few guanosines as conserved nucleotides within the sequences. Further analysis with MEME (Fig. 5C) (40), which searches for ungapped sequence motifs, also failed to identify a sequence-dependent recombination trigger (E value = 0.06). The position-dependent nucleotide probabilities (Fig. 5D) exhibit, similar to the M-COFFEE results, that guanosines are most abundant in the homologue sequences. This result gave rise to the assumption that G-C-rich sequence regions or CpG/UpU dinucleotide bias may trigger RdRp template switching, as previous studies suggest (9, 41). To evaluate this hypothesis, we compared the homologous and donor template sequences in regard to the A-U and G-C nucleotide density (Fig. 5E), the number of successive G-C and A-U base pairs (Fig. 5F), and CpG density (Fig. 5G). The analyses showed no significant differences between the donor template nucleotide composition and the sequences identified at the recombination junctions. Taken together, the limited sequence analysis results yielded no indication of any sequence-dependent recombination trigger.

DISCUSSION

Though EV-A71 infection generally causes mild diseases like HFMD in children, it can lead to severe cardiorespiratory and neurological complications (42). Intratypic recombination between circulating strains of EV-A71 and intertypic recombination with species coxsackievirus A produces the outbreak-associated strains of EV-A71, which exhibit increased virulence and/or transmissibility (15, 43). The subsequent human mortality and morbidity associated with such events can be substantial (44). All of our current understanding of recombination in the generation of new strains of enteroviruses are based upon retrospective phylogenetic analysis which shows us that recent intra- and intertypic EV-A71 recombination events are limited to members of the same species group (13, 14, 16, 42). In addition, the production of chimeric enterovirus genomes in other studies indicates a high level of plasticity (45–47). This plasticity, however, seems to be limited to intraspecies members, since no recent evidence for interspecies enterovirus recombination has been documented. Is this just due to cocirculation? Or is it due to genomic/proteomic compatibilities that are only available with other group members?

Ongoing studies using the prototypical species C enterovirus, PV, have provided unique insights into the potential triggers and mechanisms of recombination (19, 21). In general, all recent publications support the notion of replicative RdRp-mediated recombination as the primary source of new virus hybrid genome (19–21). Our major aim was to use this knowledge to develop an assay that would allow prediction of recombination between current circulating EV-A71 strains. This study reports the development of the first non-polio enterovirus recombination assay that will allow for the continued study of recombination in this medically important group of viruses. Since recombination frequencies in the closely related PV have been shown to occur at between 10^{-4} to 10^{-5} (6, 48), any impact on overall replication of the virus would impact any recombination event. Our data suggest that a minimal amount of EV-A71 recombination can occur in a process that is independent of replication and mediated by the host cell environment, potentially in a similar manner to that observed for PV by Gmyl et al. (23, 24) and other RNA viruses such as hepatitis C (35). However, we believe that our cell-based recombination assays (Fig. 1) show that recombination in EV-A71 is primarily RdRp mediated and therefore mechanistically similar to the replicative recombination observed for PV (19–21). This interpretation is supported by the results shown in Fig. 2. The L420 residue in the RdRp of PV is in a region of the polymerase that directly interacts with the viral RNA (21). This residue is conserved in EV-A71 and is located at position L421. Studies in PV have shown that a L420A mutation can inhibit

replicative recombination by ~100-fold, while having no impact upon replication (21). The same mutation in EV-A71 also produced a similar phenotype. Recombination was significantly reduced while having no impact upon replication of the full-length virus or replicon donor template (Fig. 2). The structures of the RdRp from PV and EV-A71 are very similar, and many key residues are conserved. The observation of reduced recombination from the same mutation to a similar region upon the RdRp is strongly suggestive of conservation in mechanism. In support of this, a similar mutation of the Gly-64 residue that has been shown to be important for fidelity in PV has also been engineered into EV-A71, with a similar outcome (49, 50). Current opinion proposes that enteroviruses have evolved to recombine in order to overcome the deleterious impacts of high mutation rates in order to maintain population fitness (37, 38). Or, alternatively, it may be as a consequence/by-product of replication speed (51). In either circumstance, a reduction in recombination rate should negatively impact the fitness of the viral population. The L421A mutation led to the EV-A71 population being significantly more susceptible to the nucleoside analogue mutagen ribavirin than the wild type (Fig. 2D). Again, this phenotype is conserved in PV.

We introduced additional circulating EV-A71 partners (subspecies C4 and B5) (Fig. 4). Both shared similar RNA sequence similarity to the acceptor template in the P2 and P3 regions at ~80 and ~95% at the amino acid level (Table 1). However, the phylogenetic tree (Fig. 3) of the C4 strain strongly suggests that it has evolved by genetic drift and shift (recombination). In contrast, the B5 phylogeny (Fig. 3) currently shows no evidence of shift, with evolution being limited to genetic drift only. The yield of C4/C2 recombinant was significantly lower than the C2/C2 pairing. This was not surprising since similar observations have been seen with the intertypic PV1/PV3 CRE-REP partners (20) and are presumably a reflection of the RNA sequence divergence. What cannot be explained by RNA sequence divergence is the significantly lower B5/C2 recombinant yield. Could the reduced yield with this pairing be due to lack of opportunity, i.e., distinct sites of RNA replication within the cell which decrease the likelihood of mixed replication complexes where RdRp-mediated template-switching can occur (52)? Or, could it occur as a result of a nonfunctional proteome following recombination? Potentially, recombinant RNA is being formed but may be noninfectious following packaging, i.e., the genome may be unable to replicate due to incorrect polyprotein processing or may lack suitable protein-protein interactions required for packaging (53). The latter hypothesis is somewhat supported by phylogenetic analysis of isolated circulating EV-A71 recombinant virus, which suggest functionality of the encoded polyprotein is the key determinant of viability, since recombination "hot spots" primarily localize to gene boundaries within the nonstructural region (11, 22, 42). Experimentation is under way to identify the limitations to B5/C2 recombination. However, and most importantly, these observations represent what is currently being observed in nature; the B5 strain is circulating as a pure lineage and is not associated with current recombination events.

Historical studies of circulating PV recombinant virus identified an ApU dinucleotide bias immediately prior to the recombination junction (41). Alternatively, cell-based studies have suggested that RNA structure and GC-rich regions are triggers for RdRp template switching (9). Our analyses of possible conserved sequence motifs and nucleotide composition at the identified recombination junctions yielded no indication of sequence-dependent triggers of template switching. The viable recombinant viruses that were isolated from the C4/C2 and B5/C2 recombination assays had regions of homology that were between 5 and 11 nucleotides in length (Fig. 5), which suggests that RNA sequence homology between parental partners may be important. This observation is suggestive of a "copy choice" mechanism of recombination between parental templates (6), although all historical analysis of circulating recombinant viruses are based upon evolved genomes that may not necessarily represent the primary product of recombination. Indeed, recent studies in PV suggest that recombination may be biphasic, where promiscuous sequence-independent template switching occurs that is followed by secondary selection of the most "replication-competent" viruses that show homology at the recombination junctions (20). Conceivably, the sequences we

identified from our C4/C2 intraserotypic pairing may not necessarily represent the primary product of recombination, but those that have been selected via secondary recombination events or viability. Our observations of homology at the recombination junctions are therefore consistent with the recombinant isolates observed from similar assays that have used PV as a model (20).

We believe that our described EV-A71-specific recombination assay and the results within will provide the basis for the further dissection of this key evolutionary process that may be conserved across species groups. Further, we propose that this cell-based recombination assay has some power in predicting the efficiency of recombination between the current circulating EV-A71 strains that are of public health relevance.

MATERIALS AND METHODS

Cell culture. Adherent monolayers of African green monkey (Vero) and human embryonic rhabdomyosarcoma (RD) were grown in Dulbecco modified Eagle medium. Media were supplemented with 100 U/ml penicillin, 100 µg/ml streptomycin, and 10% heat-inactivated fetal bovine serum. All cells were passaged in the presence of trypsin-EDTA. Where stated, guanidine hydrochloride (Sigma) was added to the growth medium at 4 mM. Wild-type and recombinant EV-A71 viruses were recovered after transfection of RNA generated *in vitro* (see below) from full-length cDNA or from recombination assay parental partners. Virus was quantified by PFU/ml.

Plasmids, *in vitro* transcription, cell transfection, and recombinant virus quantification. The mouse adapted EV-A71 C2-MP4 infectious clone (32) was kindly provided by Jen-Reng Wang (Cheng Kung University, Taiwan) and modified by insertion of a ribozyme sequence between the T7 promoter and viral genome sequence in a pBR-derived plasmid. The EV-A71 C2 replicon was modified from a previously described EV-A71 C2-2231 replicon (26) by the addition of a T7-ribozyme and a poly(A) sequence inserted at the 5' and 3' ends of the replicon sequence in a pBR-derived plasmid (Table 2). The EV-A71 C4 replicon was constructed from the infectious clone, which was derived from the clinical strain TW-00073-2012. Full-length genome with 5' T7/ribozyme and 3' poly(A) were amplified using PCR and cloned into the pCRII-TOPO vector (Thermo Fisher). In order to construct the replicon, a cassette consisting of the SacII restriction enzyme site and the 2Apro cleavage site was inserted into the 5'UTR/VP1 and VP4/2A boundaries, respectively. The P1 fragment of the cassette-containing plasmid was later replaced by the luciferase coding sequence by SacII restriction enzyme digestion. A similar strategy was utilized to construct the B5 infectious clone and subgenomic replicon based on the sequence of clinical strain TW-50144-2013 (22). The EV-A71Δ3D template was constructed from the full-length EV-A71 C2-MP4 infectious clone by the removal of ~800 nucleotides between the blunt-cutting restriction sites (ScaI and NruI) within the 3D^{pol} coding region. The C2-ΔIRES replicon was constructed by removal of the majority of the IRES region between two Apal restriction sites located at positions 37 and 767 of the EV-A71 C2 replicon template. The C2-L421A mutant replicon and infectious clone were constructed by site-directed mutagenesis. All primers used for plasmid construction are listed in Table 2. The EV-A71 C2 replicon and C2-ΔIRES replicon were linearized with Sall. The EV-A71-MP4 and EV-A71Δ3D cDNAs were linearized with EagI. The EV-A71 C4 and B5 replicons were linearized with NotI. All linearized cDNA was transcribed *in vitro* using T7 RNA polymerase treated with 2 U of DNase Turbo (Thermo Fisher) to remove residual DNA template. The RNA transcripts were purified by using an RNeasy minikit (Qiagen) before spectrophotometric quantification. Purified RNA in RNase-free H₂O was transfected into cell lines by using TransMessenger (Qiagen). The mixture was incubated according to the manufacturer's instructions and added to RD cell monolayers in 12-well tissue culture plates (typically 250 ng of replicon [donor] and 190 ng of Δ3D [acceptor] templates). Virus yield was quantified by plaque assay. Briefly, media, supernatant, and cells were harvested at time points posttransfection (specified in main text), subjected to three freeze-thaw cycles, and clarified. Supernatant was then used on fresh RD cells in 12-well plates, and virus infection continued for 30 min. The medium was then removed, and the cells were subjected to 2× phosphate-buffered saline (PBS; pH 7.4) washes before a 1% (wt/vol) agarose medium overlay was added. The cells were incubated for 3 to 4 days and then fixed and stained with crystal violet for virus quantification. All recombination assays were carried out in triplicate.

Ribavirin sensitivity assay. RD cells were treated with ribavirin for 3 h before infection (the doses are specified in Fig. 2). Ribavirin-treated cells were then infected at an MOI of 0.1 with either wild type or an L421A variant of EV-A71-C2-MP4 in triplicate. After infection, the cells were washed with three times with PBS, and the medium was replaced with ribavirin. Infection proceeded until a cytopathic effect (CPE) was observed. Cells and supernatant were freeze-thawed three times, the medium was clarified, and the virus was quantified by a plaque assay. Yields of virus were then normalized to a carrier-treated (dimethyl sulfoxide) control.

Single-step growth curve of the EV-A71 C4 and B5 full-length viruses. RD cells in 6-well plates were infected by each virus at an MOI of 10 in triplicate in serum-free media. One hour later, the cells were extensively washed with PBS and refreshed in 2% serum-containing medium. Virus was harvested at different time points postinfection, and the virus yield was quantified by a plaque assay.

Luciferase assays. Supernatant was removed from transfected cell monolayers, and cells were briefly washed with PBS and lysed using 100 µl of 1× Glo lysis buffer (Promega) per well in a 12-well plate. The oxidation reaction was catalyzed by the addition of 10 µl of cell lysate to 10 µl at room temperature using Bright-Glo luciferase assay system (Promega) substrate. The luciferase activity was measured using

TABLE 2 Oligonucleotides used in the study

Oligonucleotide	Sequence (5'–3') ^a
L421A-F	CTCCCTCTGCTTAGCAGCATGGCACAACG
L421A-R	CGTTGTGCCATGCTGCTAAGCAGAGGGAG
MP4 3156-F	ACGTTCTCAGTGCGGACTGTAG
C2/4 5057-R	CCTTGAAAAGAGCTTC
C4-5'UTR-SacII-2A-F	CATGCCGCGGATCACCACCTTGGTTCGCAAGTGTCCAC
C4-5'UTR-SacII-2A-R	GAACCAAGAGTGGTGTATCCGCGGCATGTTTAGCTGTATTAAG
C4-P1/P2-SacII-2A-F	TGGGCCGCGGATCACCACCTTGGGAAATTTGGACAACAGTCTG
C4-P1/P2-SacII-2A-R	AATTTCCCAAGAGTGGTGTATCCGCGGCCCAAGAGTGGTGTATCGCTG
SacII-Luc-F	ACCCCGCGGATGGAAGACGCCAAAAAC
SacII-Luc-R	TAACCGCGGCACGCGCATCTTTCCGCC
ΔP1C4-MluI-2A-F	CTTAATACAGCTAAACATGACGCGTATCACCACCTTTGG
ΔP1C4-MluI-2A-R	CCAAGAGTGGTGTATGCGCTCATGTTTAGCTGTATTAAG
B5 5'UTR-MluI-R	AATACGCGTCATGTTAATTGTATTAAGGGTC
MluI-B5-2A-F	ATGACGCGTATTACTACCCTCGGAAAGTTC
MluI-Luc-F	ACCACGCGTATGGAAGACGCCAAAAAC
MluI-Luc-R	TAAACGCGTCACGCGCATCTTTCCGCC

^aUnderscored sequences represent restriction enzyme sites used for plasmid construction.

a luminometer with values normalized to the protein content of the extract according to a protocol described previously (54).

Recombinant virus sequencing. Recombinant viruses were isolated from individual plaques by incubating the medium/agar plug overnight in 1× PBS. Viral RNA was isolated using a Qiagen viral RNA isolation kit according to the manufacturer's protocol. RNA was reverse transcribed with oligo(T) primer using Superscript II (Invitrogen) according to the manufacturer's protocol. PCR was carried from the P1 region of the acceptor template to the end of the P2 region of the donor by using Phusion high-fidelity DNA polymerase (NEB) according to the manufacturer's protocol. PCR products were gel purified, A-tailed, and subcloned into a pCRII-TOPO vector (Thermo Fisher) for sequencing. Clustal Omega was used for sequence alignment to identify recombinant junctions.

Phylogenetic analysis of the P2-P3 region of the EV-A71. The evolutionary history of EV-A71 and its relationship with CV-A16 was inferred using the neighbor-joining method and constructed in MEGA7 (55). Sequences, including 182 EV-A71 sequences and the prototype sequence of CV-A16, were analyzed and rooted with the CV-A16 prototype strain G10 isolated in 1951 (22). To specifically discriminate the recombinogenic property of different genotype/subgenotype of EV-A71, P2-P3 rather than the VP1 region was analyzed. The probability of replicate trees in which the associated taxa clustered together was determined from bootstrapped data (1,000 replicates) (56). The evolutionary distances were computed via MEGA7 using the Jukes-Cantor method and are expressed as the numbers of base substitutions per site. All positions with <95% site coverage were eliminated.

ACKNOWLEDGMENTS

C.E.C., N.H.D., and S.R.S. were funded by grant RGP0011/2015 from the Human Frontier Science Program. This research was further funded by National Institutes of Health grant R01AI45818 to C.E.C. In addition, S.R.S. was also supported by grants from the Ministry of Science and Technology (MOST), Taiwan (MOST 107-3017-F-182-001), and the Research Center for Emerging Viral Infections from The Featured Areas Research Center Program within the framework of the Higher Education Sprout Project by the Ministry of Education in Taiwan.

We thank Calvin Yeager for critical readings of the manuscript.

REFERENCES

- Hyypia T, Hovi T, Knowles NJ, Stanway G. 1997. Classification of enteroviruses based on molecular and biological properties. *J Gen Virol* 78: 1–11. <https://doi.org/10.1099/0022-1317-78-1-1>.
- Adams MJ, Lefkowitz EJ, King AMQ, Bamford DH, Breitbart M, Davison AJ, Ghabrial SA, Gorbalenya AE, Knowles NJ, Krell P, Lavigne R, Prangishvili D, Sanfacon H, Siddell SG, Simmonds P, Carstens EB. 2015. Ratification vote on taxonomic proposals to the International Committee on Taxonomy of Viruses. *Arch Virol* 160:1837–1850. <https://doi.org/10.1007/s00705-015-2425-z>.
- Cameron CE, Oh HS, Moustafa IM. 2010. Expanding knowledge of P3 proteins in the poliovirus lifecycle. *Future Microbiol* 5:867–881. <https://doi.org/10.2217/fmb.10.40>.
- Domingo E, Baranowski E, Escarmis C, Sobrino F, Holland JJ. 2002. Error frequencies of picornavirus RNA polymerases: evolutionary implications for virus populations, p 285–298. *In* Semler B, Wimmer E (ed), *Molecular Biology of Picornavirus*. ASM Press, Washington, DC. <https://doi.org/10.1128/9781555817916.ch23>.
- Vignuzzi M, Stone JK, Arnold JJ, Cameron CE, Andino R. 2006. Quasispecies diversity determines pathogenesis through cooperative interactions in a viral population. *Nature* 439:344–348. <https://doi.org/10.1038/nature04388>.
- Kirkegaard K, Baltimore D. 1986. The mechanism of RNA recombination in poliovirus. *Cell* 47:433–443. [https://doi.org/10.1016/0092-8674\(86\)90600-8](https://doi.org/10.1016/0092-8674(86)90600-8).
- Lai MMC. 1992. Genetic recombination in RNA viruses. *Curr Top Microbiol Immunol* 176:21–32.

8. Cooper PD, Steiner-Pryor A, Scotti PD, DeLong D. 1974. Nature of poliovirus genetic recombinants. *J Gen Virol* 23:41–49. <https://doi.org/10.1099/0022-1317-23-1-41>.
9. Runckel C, Westesson O, Andino R, DeRisi JL. 2013. Identification and manipulation of the molecular determinants influencing poliovirus recombination. *PLoS Pathog* 9(2):e1003164. <https://doi.org/10.1371/journal.ppat.1003164>.
10. Shih SR, Stollar V, Li ML. 2011. Host factors in enterovirus 71 replication. *J Virol* 85:9658–9666. <https://doi.org/10.1128/JVI.05063-11>.
11. Zhang C, Zhu R, Yang Y, Chi Y, Yin J, Tang X, Yu L, Zhang C, Huang Z, Zhou D. 2015. Phylogenetic analysis of the major causative agents of hand, foot, and mouth disease in Suzhou City, Jiangsu province, China, in 2012–2013. *Emerg Microbes Infect* 4:e12. <https://doi.org/10.1038/emi.2015.12>.
12. McWilliam Leitch EC, Cabrero M, Cardoso J, Harvala H, Ivanova OE, Koike S, Kroes AC, Lukashev A, Perera D, Roivainen M, Susi P, Trallero G, Evans DJ, Simmonds P. 2012. The association of recombination events in the founding and emergence of subgenogroup evolutionary lineages of human enterovirus 71. *J Virol* 86:2676–2685. <https://doi.org/10.1128/JVI.06065-11>.
13. Li L, He Y, Yang H, Zhu J, Xu X, Dong J, Zhu Y, Jin Q. 2005. Genetic characteristics of human enterovirus 71 and coxsackievirus A16 circulating from 1999 to 2004 in Shenzhen, People's Republic of China. *J Clin Microbiol* 43:3835–3839. <https://doi.org/10.1128/JCM.43.8.3835-3839.2005>.
14. Ang LW, Koh BK, Chan KP, Chua LT, James L, Goh KT. 2009. Epidemiology and control of hand, foot and mouth disease in Singapore, 2001–2007. *Ann Acad Med Singapore* 38:106–112.
15. Liu W, Wu S, Xiong Y, Li T, Wen Z, Yan M, Qin K, Liu Y, Wu J. 2014. Co-circulation and genomic recombination of coxsackievirus A16 and enterovirus 71 during a large outbreak of hand, foot, and mouth disease in Central China. *PLoS One* 9:e96051. <https://doi.org/10.1371/journal.pone.0096051>.
16. Zhang Y, Zhu Z, Yang W, Ren J, Tan X, Wang Y, Mao N, Xu S, Zhu S, Cui A, Zhang Y, Yan D, Li Q, Dong X, Zhang J, Zhao Y, Wan J, Feng Z, Sun J, Wang S, Li D, Xu W. 2010. An emerging recombinant human enterovirus 71 responsible for the 2008 outbreak of hand foot and mouth disease in Fuyang City of China. *Virol J* 7:94. <https://doi.org/10.1186/1743-422X-7-94>.
17. Leitch ECM, Bendig J, Cabrero M, Cardoso J, Hyypia T, Ivanova OE, Kelly A, Kroes ACM, Lukashev A, MacAdam A, McMinn P, Roivainen M, Trallero G, Evans DJ, Simmonds P. 2009. Transmission networks and population turnover of echovirus 30. *J Virol* 83:2109–2118. <https://doi.org/10.1128/JVI.02109-08>.
18. McWilliam Leitch EC, Cabrero M, Cardoso J, Harvala H, Ivanova OE, Kroes ACM, Lukashev A, Muir P, Odoo J, Roivainen M, Susi P, Trallero G, Evans DJ, Simmonds P. 2010. Evolutionary dynamics and temporal/geographical correlates of recombination in the human enterovirus echovirus types 9, 11, and 30. *J Virol* 84:9292–9300. <https://doi.org/10.1128/JVI.00783-10>.
19. Woodman A, Arnold JJ, Cameron CE, Evans DJ. 2016. Biochemical and genetic analysis of the role of the viral polymerase in enterovirus recombination. *Nucleic Acids Res* 44:6883–6895. <https://doi.org/10.1093/nar/gkw567>.
20. Lowry K, Woodman A, Cook J, Evans DJ. 2014. Recombination in enteroviruses is a biphasic replicative process involving the generation of greater-than genome length 'imprecise' intermediates. *PLoS Pathog* 10(6):e1004191. <https://doi.org/10.1371/journal.ppat.1004191>.
21. Kempf BJ, Peersen OB, Barton DJ. 2016. Poliovirus polymerase Leu420 facilitates RNA recombination and ribavirin resistance. *J Virol* 90:8410–8421. <https://doi.org/10.1128/JVI.00078-16>.
22. Lee KM, Gong YN, Hsieh TH, Woodman A, Dekker NH, Cameron CE, Shih SR. 2018. Discovery of enterovirus A71-like nonstructural genomes in recent circulating viruses of the enterovirus A species. *Emerg Microbes Infect* 7:111. <https://doi.org/10.1038/s41426-018-0107-0>.
23. Gmyl AP, Belousov EV, Maslova SV, Khitrina EV, Chetverin AB, Agol VI. 1999. Nonreplicative RNA recombination in poliovirus. *J Virol* 73:8958–8965.
24. Gmyl AP, Korshenko SA, Belousov EV, Khitrina EV, Agol VI. 2003. Non-replicative homologous RNA recombination: promiscuous joining of RNA pieces? *RNA* 9:1221–1231. <https://doi.org/10.1261/rna.5111803>.
25. Woodman A, Lee K-M, Janissen R, Gong Y-N, Shih S-R, Dekker NH, Cameron CE. 2018. Predicting intra- and intertypic recombination in enterovirus 71. *bioRxiv* <https://doi.org/10.1101/445783>.
26. Tang WF, Huang RT, Chien KY, Huang JY, Lau KS, Jheng JR, Chiu CH, Wu TY, Chen CY, Horng JT. 2016. Host microRNA miR-197 plays a negative regulatory role in the enterovirus 71 infectious cycle by targeting the RAN protein. *J Virol* 90:1424–1438. <https://doi.org/10.1128/JVI.02143-15>.
27. Herold J, Andino R. 2000. Poliovirus requires a precise 5' end for efficient positive-strand RNA synthesis. *J Virol* 74:6394–6400. <https://doi.org/10.1128/JVI.74.14.6394-6400.2000>.
28. Goodfellow IG, Kerrigan D, Evans DJ. 2003. Structure and function analysis of the poliovirus cis-acting replication element (CRE). *RNA* 9:124–137. <https://doi.org/10.1261/rna.2950603>.
29. Goodfellow IG, Polacek C, Andino R, Evans DJ. 2003. The poliovirus 2C cis-acting replication element-mediated uridylylation of VPg is not required for synthesis of negative-sense genomes. *J Gen Virol* 84:2359–2363. <https://doi.org/10.1099/vir.0.19132-0>.
30. Smithee S, Tracy S, Chapman NM. 2015. Mutational disruption of cis-acting replication element 2C in coxsackievirus B3 leads to 5'-terminal genomic deletions. *J Virol* 89:11761–11772. <https://doi.org/10.1128/JVI.01308-15>.
31. Smithee S, Tracy S, Chapman NM. 2016. Reversion to wild type of a mutated and nonfunctional coxsackievirus B3CRE(2C). *Virus Res* 220:136–149. <https://doi.org/10.1016/j.virusres.2016.04.016>.
32. Wang YF, Chou CT, Lei HY, Liu CC, Wang SM, Yan JJ, Su JJ, Wang JR, Yeh TM, Chen SH, Yu CK. 2004. A mouse-adapted enterovirus 71 strain causes neurological disease in mice after oral infection. *J Virol* 78:7916–7924. <https://doi.org/10.1128/JVI.78.15.7916-7924.2004>.
33. Yamayoshi S, Fujii K, Koike S. 2014. Receptors for enterovirus 71. *Emerg Microbes Infect* 3:e53. <https://doi.org/10.1038/emi.2014.49>.
34. Gmyl AP, Korshenko SA, Belousov EV, Khitrina EV, Agol VI. 2003. Non-replicative homologous RNA recombination: promiscuous joining of RNA pieces? *RNA* 9:1221–1231. <https://doi.org/10.1261/rna.5111803>.
35. Scheel TKH, Galli A, Li Y-P, Mikkelsen LS, Gottwein JM, Bukh J. 2013. Productive homologous and non-homologous recombination of hepatitis C virus in cell culture. *PLoS Pathog* 9(3):e1003228. <https://doi.org/10.1371/journal.ppat.1003228>.
36. Gallei A, Pankraz A, Thiel HJ, Becher P. 2004. RNA recombination *in vivo* in the absence of viral replication. *J Virol* 78:6271–6281. <https://doi.org/10.1128/JVI.78.12.6271-6281.2004>.
37. Muller HJ. 1964. The relation of recombination to mutational advance. *Mutat Res* 1:2–9. [https://doi.org/10.1016/0027-5107\(64\)90047-8](https://doi.org/10.1016/0027-5107(64)90047-8).
38. Simon-Loriere E, Holmes EC. 2011. Why do RNA viruses recombine? *Nat Rev Microbiol* 9:617–626. <https://doi.org/10.1038/nrmicro2614>.
39. Moretti S, Armogom F, Wallace IM, Higgins DG, Jongeneel CV, Notredame C. 2007. The M-Coffee web server: a meta-method for computing multiple sequence alignments by combining alternative alignment methods. *Nucleic Acids Res* 35:W645–W648. <https://doi.org/10.1093/nar/gkm333>.
40. Bailey TL, Boden M, Buske FA, Frith M, Grant CE, Clementi L, Ren JY, Li WW, Noble WS. 2009. MEME SUITE: tools for motif discovery and searching. *Nucleic Acids Res* 37:W202–W208. <https://doi.org/10.1093/nar/gkp335>.
41. Kew O, Morris-Glasgow V, Landaverde M, Burns C, Shaw J, Garib Z, Andre J, Blackman E, Freeman CJ, Jorba J, Sutter R, Tambini G, Venczel L, Pedreira C, Laender F, Shimizu H, Yoneyama T, Miyamura T, van der Avoort H, Oberste MS, Kilpatrick D, Cochi S, Pallansch M, de Quadros C. 2002. Outbreak of poliomyelitis in Hispaniola associated with circulating type 1 vaccine-derived poliovirus. *Science* 296:356–359. <https://doi.org/10.1126/science.1068284>.
42. Yip CC, Lau SK, Lo JY, Chan KH, Woo PC, Yuen KY. 2013. Genetic characterization of EV71 isolates from 2004 to 2010 reveals predominance and persistent circulation of the newly proposed genotype D and recent emergence of a distinct lineage of subgenotype C2 in Hong Kong. *Virol J* 10:222. <https://doi.org/10.1186/1743-422X-10-222>.
43. Huang SC, Hsu YW, Wang HC, Huang SW, Kiang D, Tsai HP, Wang SM, Liu CC, Lin KH, Su JJ, Wang JR. 2008. Appearance of intratypic recombination of enterovirus 71 in Taiwan from 2002 to 2005. *Virus Res* 131:250–259. <https://doi.org/10.1016/j.virusres.2007.10.002>.
44. Gan ZK, Jin H, Li JX, Yao XJ, Zhou Y, Zhang XF, Zhu FC. 2015. Disease burden of enterovirus 71 in rural central China: a community-based survey. *Hum Vaccin Immunother* 11:2400–2405. <https://doi.org/10.1080/21645515.2015.1059980>.
45. Combelas N, Holmblat B, Joffret M-L, Colbere-Garapin F, Delpeyroux F. 2011. Recombination between poliovirus and coxsackie A viruses of species C: a model of viral genetic plasticity and emergence. *Viruses* 3:1460–1484. <https://doi.org/10.3390/v3081460>.

46. Bessaud M, Joffret ML, Blondel B, Delpeyroux F. 2016. Exchanges of genomic domains between poliovirus and other cocirculating species C enteroviruses reveal a high degree of plasticity. *Sci Rep* 6:38831. <https://doi.org/10.1038/srep38831>.
47. Jiang P, Faase JA, Toyoda H, Paul A, Wimmer E, Gorbalenya AE. 2007. Evidence for emergence of diverse polioviruses from C-cluster coxsackie A viruses and implications for global poliovirus eradication. *Proc Natl Acad Sci U S A* 104:9457–9462. <https://doi.org/10.1073/pnas.0700451104>.
48. Kirkegaard K, Baltimore D. 1986. RNA recombination in poliovirus. *J Cell Biochem* 1986:289–289.
49. Meng T, Kwang J. 2014. Attenuation of human enterovirus 71 high-replication-fidelity variants in AG129 mice. *J Virol* 88:5803–5815. <https://doi.org/10.1128/JVI.00289-14>.
50. Sadeghipour S, Bek EJ, McMinn PC. 2013. Ribavirin-resistant mutants of human enterovirus 71 express a high replication fidelity phenotype during growth in cell culture. *J Virol* 87:1759–1769. <https://doi.org/10.1128/JVI.02139-12>.
51. Fitzsimmons WJ, Woods RJ, McCrone JT, Woodman A, Arnold JJ, Yenawar M, Evans R, Cameron CE, Lauring AS. 2018. A speed-fidelity trade-off determines the mutation rate and virulence of an RNA virus. *PLoS Biol* 16(6):e2006459. <https://doi.org/10.1371/journal.pbio.2006459>.
52. Egger D, Bienz K. 2002. Recombination of poliovirus RNA proceeds in mixed replication complexes originating from distinct replication start sites. *J Virol* 76:10960–10971. <https://doi.org/10.1128/JVI.76.21.10960-10971.2002>.
53. Liu Y, Wang C, Mueller S, Paul AV, Wimmer E, Jiang P. 2010. Direct interaction between two viral proteins, the nonstructural protein 2C(ATPase) and the capsid protein VP3, is required for enterovirus morphogenesis. *PLoS Pathog* 6(8):e1001066. <https://doi.org/10.1371/journal.ppat.1001066>.
54. Weeks SA, Lee CA, Zhao Y, Smidansky ED, August A, Arnold JJ, Cameron CE. 2012. A polymerase mechanism-based strategy for viral attenuation and vaccine development. *J Biol Chem* 287:31618–31622. <https://doi.org/10.1074/jbc.C112.401471>.
55. Kumar S, Stecher G, Tamura K. 2016. MEGA7: molecular evolutionary genetics analysis version 7.0 for bigger datasets. *Mol Biol Evol* 33:1870–1874. <https://doi.org/10.1093/molbev/msw054>.
56. Felsenstein J. 1985. Confidence limits on phylogenies: an approach using the bootstrap. *Evolution* 39:783–791. <https://doi.org/10.2307/2408678>.